中国光学 Chinese Optics 核心期刊

金属接触对有机薄膜激光特性的影响

郝亚茹 邓招奇

The effects of metallic contacts on the lasing characteristics of organic thin films

HAO Ya-ru, DENG Zhao-qi

引用本文:
郝亚茹, 邓招奇. 金属接触对有机薄膜激光特性的影响[J]. 中国光学, 2020, 13(4): 866–872. doi: 10.37188/CO.2020–0007
HAO Ya-ru, DENG Zhao-qi. The effects of metallic contacts on the lasing characteristics of organic thin films[J]. *Chinese Optics*, 2020, 13(4): 866-872. doi: 10.37188/CO.2020-0007

在线阅读 View online: https://doi.org/10.37188/CO.2020–0007

文章编号 2095-1531(2020)04-0866-07

The effects of metallic contacts on the lasing characteristics of organic thin films

HAO Ya-ru, DENG Zhao-qi*
(*University of Electronic Science and Technology of China, Zhongshan Institute, Zhongshan* 528402, *China*)
* *Corresponding author, E-mail: yeyunxiaopan@foxmail.com*

Abstract: Optical loss caused by metallic contacts are thought to be a major obstacle to the achievement of organic laser diodes. We find that multi-channel emissions and Surface Plasmons (SPs) by designing a proper distributed feedback structure can allow successful lasing in organic thin films in the presence of contacting electrodes and even show better lasing performance when compared to metal-free cases. In this paper, a lower threshold (0.026 mJ/pulse) laser emission is achieved with the Ag metal electrode on the grating structure with a period of 740 nm. Since there is no increase in device thickness, the electrical properties are not reduced when the optical properties are improved.
Key words: organic laser; surface plasmons; grating coupling

金属接触对有机薄膜激光特性的影响

郝亚茹,邓招奇*
(电子科技大学中山学院,广东 中山 528402)

摘要:金属触点引起的光学损耗被认为是阻碍电泵浦有机激光器发展的主要障碍。本文对于存在金属接触电极的有机薄膜,通过设计适当的分布反馈结构形成多通道发射和表面等离子体激元(SPs),从而实现光泵浦激光。与采用无金属接触电极的有机薄膜进行对比,结果表明,本文方法可实现更好的激光性能。利用本文设计的结构,在 740 nm 光栅结构的 Ag 衬底上实现了 (0.026 mJ/pulse) 的激光发射。由于本文设计方法没有增加器件厚度,所以当光学性能得到改善时,电性能并没有降低。
关 键 词:有机激光;表面等离子体;光栅耦合
中图分类号:O439 **文献标志码:**A **doi:**10.37188/CO.2020-0007

收稿日期:2020-01-10; **修订日期:**2020-03-09
基金项目:国家自然科学基金(No.61605083);中山市重大专项(No.2017B1023)
Supported by National Natural Science Foundation of China (No.61605083); Major Projects in Zhongshan City (No.2017B1023)

1 Introduction

Since the discovery of high optical-gain and stimulated-emission properties in organic thin films from small molecules and polymers[1-3], Organic Semiconductor Lasers (OSLs) have been extensively explored due to their broad wavelength tunability throughout the visible spectrum[4-5] and their potential for low-cost fabrication[6-7]. To date, although classic laser devices have been applied in chemistry[8-9], biology[10], physics[11], and many other fields[12-15], it is not yet possible to obtain stimulated emission from electrical pumping[16-17]. A major obstacle to achieving this is the need to include a metallic electrode in close proximity to the gain medium for charge carrier injection. This is a problem because of the optical loss arising from metallic contacts generally outweighs the optical gain. Previous attempts to study lasing action in organic materials in the presence of an electrode layer have shown a substantial rise in lasing threshold[18]. Reufer *et al*[19]. have demonstrated a way in which a metal contact can be applied without increasing the threshold by increasing the thickness of the polymer layer because, as they pointed out, the losses depend on the electric field distribution through the polymer layer. Increasing polymer thickness reduces the strength of the electric field at the metal contact, thereby reducing the associated losses. However, this leads to another problem: the amount of current that could be passed through the device is limited by the thicker polymer film due to charge injection and transportation problems. A balance needs to be achieved between threshold and current by tuning the thickness of devices carefully, or it is necessary to give up this idea and find another way in which the threshold can be reduced without increasing the polymer's thickness. The utilization of SPs may be a wise choice[20-21].

2 Experimental methods

SPs have been widely utilized to couple light through the metal electrode layer in Organic Light-Emitting Diodes (OLEDs) to enhance their emission properties[11-13]. For a given frequency ω and the dielectric constant ε_M and ε_D (ε_D=1 for air) for the metal and the dielectric, the dispersion for an SPs is given by

$$k_{sp} = \frac{\omega}{c}\sqrt{\frac{\varepsilon_M \varepsilon_D}{\varepsilon_M + \varepsilon_D}}, \qquad (1)$$

where k_{sp} is the wave vector component of the SPs parallel to the surface. In the structures of OLEDs, not all of the light emitted in the organic layer emerges because much of it is trapped by the guided modes of their structure, including the SPs modes associated with electrode/organic interface. In order to improve device efficiency, their wavelength scale periodic microstructures have been introduced to allow coupling of the SPs modes to light[22-23]. The OSLs have similar problems since the metallic electrode is unavoidable for electrical operation and the loss of absorption by the electrode will increase the lasing threshold. Therefore, it can be concluded that the SPs should be excited to offset the negative effects caused by electrode absorption without reducing their electrical efficiency (e.g. increasing the thickness of devices).

In this paper, we show that SPs can minimize the interaction between the gain mode and the quenching channel of electrodes. We can achieve a fully contacted laser structure with a mere 10% increase in the lasing threshold by using multi-channel emission, and we demonstrate that the choice of a proper metallic layer can even lead to a reduction in threshold with the help of the SPs.

The K9 glass substrate grating was prepared holographically in a photoresist and then dry-etched. It had a depth of 60 nm and a period of 740 nm. A 30-nm thick metal layer was fabricated using

thermal evaporation in a high-vacuum system with a base pressure of less than 5×10^{-4} Pa without breaking the vacuum. An Atomic Force Microscope (AFM) image of the substrate is shown in Fig. 1.

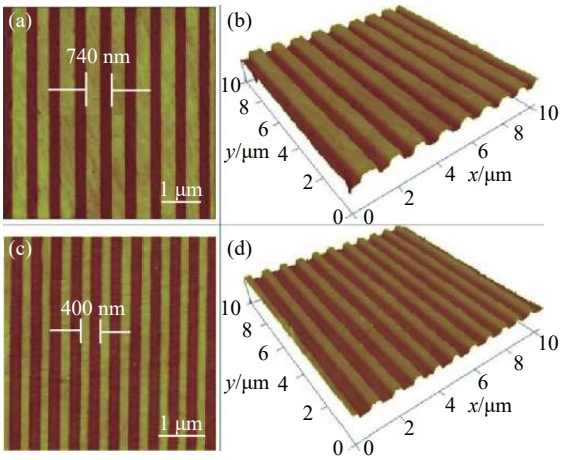

Fig. 1 The grating structure scanned with an atomic force microscope

For comparison, a quartz substrate without periodical corrugation has also been used. Red fluorescence dye 4-(dicyanomethylene)-2-isopropyl-6-(1,1,7,7-tetramethyljulolidyl-9-enyl)-4h-pyran (DCJTI) was used as the emissive dopant in poly(N-vinylcarbazole) (PVK) and then spic-coated with chlorobenzene. The doping concentration was approximately 2% (by weight). The resulting absorption and photoluminescence spectra are shown in Fig. 2. The average film thickness was about 300 nm. Here, we choose PVK as the film-forming material since its refractive index allows the whole device's parameters to satisfy the Bragg condition. The laser structures were optically pumped by a frequency-tripled Nd-YAG laser (Spectra-Physics) at λ_p=355 nm with a 10 Hz repetition rate and 5 ns pulses.

The output pulse energy of the pump laser was controlled using neutral-density filters. An adjustable slit and a cylindrical lens were used before the beam splitter to shape the beam into a narrow stripe with varying length on the sample film. The films were pumped at an angle incidence with the long axis of the pump beam perpendicular to the groove of the grating. The output signals were detected by a fiber-coupled CCD spectrometer (JY Spex CCD3 000). The pumped energies from the laser were measured using a calibrated laser power and energy meter (Gentec).

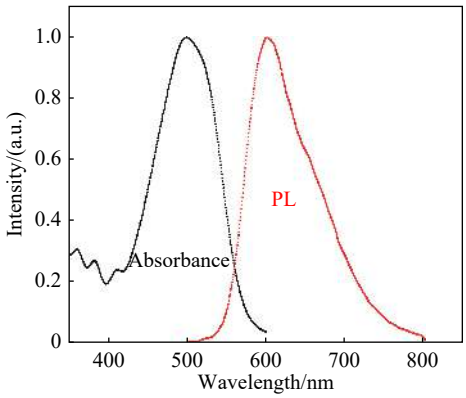

Fig. 2 Absorption and photoluminescence spectra of the DCJTI:PVK film

3 Results and discussion

The characteristics of the red multi-beam laser are shown in Fig. 3. The photographs of the far-field pattern are shown in the inset, from which one can see laser emissions along ±53° with a grating period of 740 nm, and +28° or −56° with a grating period of 400 nm. Table 1 summarizes the threshold values of devices with a flat substrate and periodical substrate (400 nm and 740 nm) as well as different metal layers. As for the flat quartz substrate, we can see that the Amplified Spontaneous Emission (ASE) threshold of the metal-free device is 0.057 mJ/pulse. In comparison, when the gain materials are spin-coated onto the metal layers, the ASE threshold increases dramatically at 0.37 mJ/pulse with an Al layer and 0.41 mJ/pulse with an Ag layer.

If we spin-coat the gain medium onto the periodical substrate with Λ of 400 nm, which satisfies the second-order Bragg condition, the lasing threshold also increases when adding metal layers onto the substrate. However, when a periodical substrate with Λ of 740 nm is utilized, which satisfies the fourth-order Bragg condition, the threshold of

the Al-backed device is 0.067 mJ/pulse. This is a mere 10% increase with respect to the 0.06 mJ/pulse threshold of the metal-free device. The threshold of the Ag-backed device decreases to 0.026 mJ/pulse.

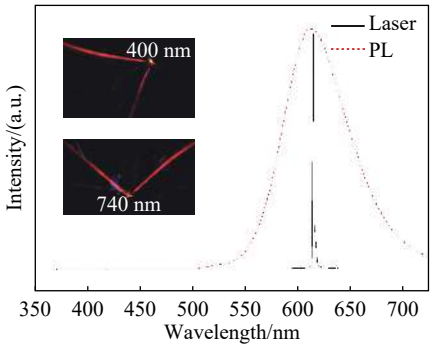

Fig. 3　Emission spectra of DCJTI:PVK system pumped with an optically pulsed laser at above the lasing threshold. The inset shows the photograph of the far-field pattern.

Tab. 1　ASE characteristics of DCJTI:PVK films with quartz substrate and lasing characteristics of distributed feedback lasers (gain material DCJTI:PVK) with grating period of 400 nm and 740 nm.

Metal layer	Period /nm	Threshold /(mJ·pulse^{-1})	Wavelength /nm	FWHM /nm
(none)	(flat substrate)	0.057	635	12.4
Al	(flat substrate)	0.37	632	11.8
Ag	(flat substrate)	0.41	632	12.1
(none)	400	0.03	641	0.13
Al	400	0.13	637	0.15
Ag	400	0.16	640	0.23
(none)	740	0.06	613	0.32
Al	740	0.067	612	0.25
Ag	740	0.026	615	0.37

As shown in Table 1, the FWHMs of the devices with a grating period of 740 nm are larger than those with a period of 400 nm despite their lower lasing thresholds. Compared to the device with a grating period of 400 nm, the lower threshold of the one with a period of 740 nm is due to the excitation of the SPs, and the larger FWHM of the latter is due to the frequency selection effect of the grating.

In order to understand these results, the grating coupling condition should be considered:

$$k_{\mathrm{WG},z} \pm l k_{\mathrm{g}} = k_{\mathrm{laser},z}, \qquad (2)$$

Where $k_{\mathrm{WG},z} = k_0 n_f \sin\alpha = k_0 n_{\mathrm{eff}}$ is the z-directional guided mode wave vector, $k_{\mathrm{g}} = \dfrac{2\pi}{\Lambda}$ is the grating vector, $k_{\mathrm{laser},z} = k_0 \sin\theta_l$, is the z-directional laser light wave vector, θ_l is the emission angle, and l is an integer. According to equation (2), the DCJTI:PVK laser coupling is determined. From the inset in Fig. 4, when Λ=740 nm, the forward mode can couple into θ_{-1} =55.47°, θ_{-2} = −0.25° and θ_{-3} =−56.39° emission angles due to the grating coupling condition, which is occurs when $l = -1$, $l = -2$, $l = -3$, respectively. Meanwhile, the backward mode can emit into very similar (theoretically equal) angles at θ_1 = −56.39°, θ_2 = 0.25°, θ_3 = 55.47°.

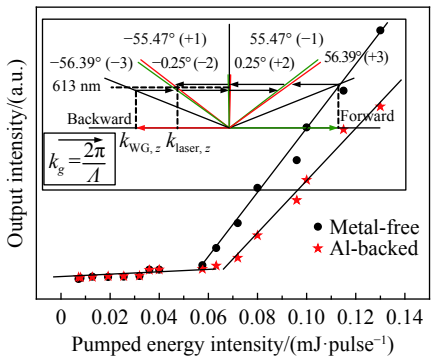

Fig. 4　Output emission intensity integrated over all wavelengths as a function of the pump intensity for metal-free device (circles); DCJTI:PVK films with quartz substrate and Al-backed device (stars); DCJTI:PVK films with a grating period of 740 nm. The inset shows the grating coupling processes between the waveguide mode and lasing emission under the fourth Bragg condition

The coupling between the forward and backward modes forms the multi-beam laser emission. In other words, a multi-output channel has been established, which can minimize the interaction between the gain mode and the quenching channel of the electrodes. Therefore, as shown in Fig. 4 (color online), the Al-backed device with Λ=740 nm has similar

properties to the metal-free one. However, as for Λ= 400 nm, the coupling between the forward and backward modes forms the single-beam laser emission at angle $\theta_{-1} = 0.2°$ and $\theta_1 = -0.2°$, meaning that there is no multi-output channel and the interaction between the gain mode and the quenching channel of the electrodes is large. Similar to the flat substrate, the threshold of a metal-backed device with Λ=400 nm is larger than the threshold of that without metal.

From Fig. 5, there is a novel phenomenon that the Ag-backed device with Λ of 740 nm shows a smaller laser threshold than the metal-free one. We believe that the key is the SPs offset loss caused by electrode absorption. Similar to OLEDs, the dispersion for SPs from the electrode/organic interface in OSLs can be calculated using equation (1). This is arguably even more complex due to the directional properties of OSLs. However, with careful control, we can couple the SPs modes to the lasing light. Then, the excitation condition is satisfied by,

$$k_{sp} = n_{eff}\frac{2\pi}{\lambda}\sin\theta_l \pm lk_g, \qquad (3)$$

where n_{eff} is the effective refractive index of the DCJTI:PVK organic film, $k_g = \frac{2\pi}{\Lambda}$ is the grating vector (when the grating period Λ is 740 nm), k_{sp} is the wave vector component of the SPs mode and l is an integer. The SPs modes decay by emitting light according to the grating coupling condition of the SPs modes into air,

$$k_{sp} = \frac{2\pi}{\lambda}\sin\beta_m \pm m\frac{2\pi}{\Lambda}, \qquad (4)$$

where β is the emission angle and m is the order of grating coupling. Then, according to equation (3) and (4), we get that the SPs of the Ag-backed device with Λ of 740 nm can exit at angle $\theta = -28.35°$ and emit at angle $\beta = 55.78°$ (close to the laser emission angle), which are summarized in the inset of Fig. 5. We have observed subtle differences in spectra with and without SPs but significant differences in the output polarization.

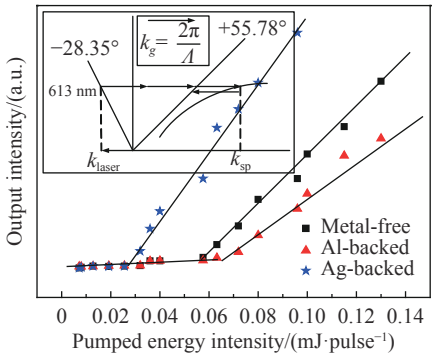

Fig. 5 Output emission intensity integrated over all wavelengths as a function of the pump intensity for metal-free device (rectangles); DCJTI:PVK films with quartz substrate, Al-backed device (triangles); DCJTI:PVK films and Ag-backed device (stars); DCJTI:PVK films with a grating period of 740 nm. The inset shows the exiting and coupling processes between the lasing light and the SPs mode

In the absence of SPs, the ratio of light polarized parallel to the grating groove to light polarized perpendicular to the grating groove is 200∶1. This ratio decreases to 4∶1 in presence of SPs. This shows that the SPs exited through the coupling toward the emission direction of the Ag-backed device with Λ of 740 nm, which should be attributed to the reduction of the lasing threshold. As for the Al-backed device with Λ of 740 nm, since the SPs cannot be coupled out to the lasing emission direction according to equations (3) and (4), the threshold is similar to the metal-free one. As for Λ=400 nm, there were no multi-channel and coupling SPs in metal-free and metal-backed devices.

In general, excited SPs influence the electric field distribution in the grating. To further study the coupling between SPs and laser emission, a Finite-Difference Time-Domain (FDTD) simulation was performed and the Maxwell equations were solved numerically. The grating structure was modeled in FDTD (Numerical FDTD Solutions 2018), with constraints imposed by interface matching and periodic boundary conditions. Figure 6 shows the electric field intensity distribution at normal incidence obtained by FDTD simulations for the DCJTI:PVK

DFB laser with an Ag thickness of 30 nm. It can be seen that at the DCJTI: PVK / Ag interface, large photon energy of 1.97 eV (615 nm) can be established, which indicates that SPs become excited.

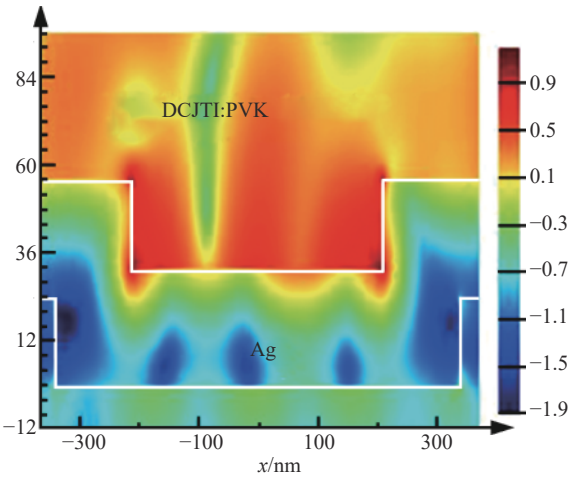

Fig. 6　Simulations for the excited SPs intensity from the DCJTI:PVK DFB laser with Ag layer thickness of 30 nm

4　Conclusions

In summary, compared to the ASE on a common substrate without a periodical structure, we have achieved a lower threshold organic laser emission on a grating substrate where contact losses are caused by a metal electrode. However, different grating structures and different metal electrodes influence the performance of the laser properties. The study shows that a lower threshold (0.026 mJ/pulse) laser emission occurs with the Ag metal electrode on a grating structure with a period of 740 nm, which is due to the combined effect of the periodic multichannel emission and the excited SPs of the Ag layer. In comparison, there are no excited SPs on a grating structure with a period of 400 nm, so the threshold is shown to be higher (0.16 mJ/pulse). However, when a metal-free substrate is applied, it once again has a low threshold. Meanwhile, the introduction of an Al metal electrode does not excite SPs on the grating structure, so the threshold must be higher (0.067 mJ/pulse). Our results show that by properly adjusting the grating structure and metal electrodes, optical losses associated with metallic contacts can be overcome.

参考文献:

[1] QIAN SH X, SNOW J B, TZENG H M, *et al*.. Lasing droplets: highlighting the liquid-air interface by laser emission[J]. *Science*, 1986, 231(4737): 486-488.

[2] KALLINGER C, HILMER M, HAUGENEDER A, *et al*.. A flexible conjugated polymer laser[J]. *Advanced Materials*, 1998, 10(12): 920-923.

[3] FROLOV S V, VARDENY Z V, YOSHINO K. Cooperative and stimulated emission in poly (*p*-phenylene-vinylene) thin films and solutions[J]. *Physical Review B*, 1998, 57(15): 9141-9147.

[4] 张镭, 杨杨, 高劼超, 等. 有机材料EnBOD的放大自发发射性能研究[J]. 发光学报, 2015, 36(6): 661-665.
ZHANG L, YANG Y, GAO J CH, *et al*.. Study on Amplified Spontaneous Emission Properties of En BOD material[J]. *Chinese Journal of Luminescence*, 2015, 36(6): 661-665. (in Chinese)

[5] GROSSMANN T, WIENHOLD T, BOG U, *et al*.. Polymeric photonic molecule super-mode lasers on silicon[J]. *Light*: *Science* & *Applications*, 2013, 2(5): e82.

[6] 张镭, 李颜涛, 林杰, 等. 基于Alq：DCJTI薄膜的光泵浦650nm微腔激光[J]. 发光学报, 2015, 36(9): 1059-1063.
ZHANG L, LI Y T, LIN J, *et al*.. Microcavity lasing at 650 nm from Alq：DCJTI film under optical pumping[J]. *Chinese Journal of Luminescence*, 2015, 36(9): 1059-1063. (in Chinese)

[7] CHEN SH M, LI K F, LI G X, *et al*.. Gigantic electric-field-induced second harmonic generation from an organic conjugated polymer enhanced by a band-edge effect[J]. *Light*: *Science* & *Applications*, 2019, 8(1): 17.

[8] 付东旭, 郑令娜, 刘金辉, 等. 激光剥蚀-电感耦合等离子体质谱定量分析单细胞中的银纳米颗粒[J]. 分析化学, 2019, 47(9): 1390-1394.
FU D X, ZHENG L N, LIU J H, *et al*.. Quantitative analysis of silver nanoparticles in single cell by laser ablation inductively coupled plasma-mass spectrometry[J]. *Chinese Journal of Analytical Chemistry*, 2019, 47(9): 1390-

1394.(in Chinese)
[9] 孙兰香, 汪为, 田雪咏, 等. 激光诱导击穿光谱微区分析的研究应用进展[J]. 分析化学, 2018, 46(10): 1518-1527.
SUN L X, WANG W, TIAN X Y, *et al*.. Progress in research and application of micro-laser-induced breakdown spectroscopy[J]. *Chinese Journal of Analytical Chemistry*, 2018, 46(10): 1518-1527. (in Chinese)
[10] LETOKHOV V S. Laser biology and medicine[J]. *Nature*, 1985, 316(6026): 325-330.
[11] MOUROU G A, BARTY C P, PERRY M D. Ultrahigh-intensity laser: physics of the extreme on a tabletop[R]. Washington, DC: Lawrence Livermore National Lab, 1997.
[12] BRANCALEON L, MOSELEY H. Laser and non-laser light sources for photodynamic therapy[J]. *Lasers in Medical Science*, 2002, 17(3): 173-186.
[13] 饶刚福, 黄林, 刘木华, 等. 基于激光诱导击穿光谱的微生物种类鉴别研究[J]. 分析化学, 2018, 46(7): 1122-1128.
RAO G F, HUANG L, LIU M H, *et al*.. Discrimination of microbe species by laser induced breakdown spectroscopy[J]. *Chinese Journal of Analytical Chemistry*, 2018, 46(7): 1122-1128. (in Chinese)
[14] 喻佳俊, 刘平, 曾真, 等. 直线式基质辅助激光解吸电离质谱仪的研制与性能表征[J]. 分析化学, 2018, 46(4): 463-470.
YU J J, LIU P, ZENG ZH, *et al*.. Development and characterization of a linear matrix-assisted laser desorption ionization mass spectrometer[J]. *Chinese Journal of Analytical Chemistry*, 2018, 46(4): 463-470. (in Chinese)
[15] 邓文婵, 韩国斌, 李原芳, 等. 基质辅助激光解析/电离质谱用于呼吸道合胞病毒感染细胞的差异性分析[J]. 分析化学, 2018, 46(2): 165-169.
DENG W CH, HAN G B, LI Y F, *et al*.. Distinction of cells infected with respiratory syncytial virus by matrix assisted laser desorption/ionization mass spectrometry[J]. *Chinese Journal of Analytical Chemistry*, 2018, 46(2): 165-169. (in Chinese)
[16] KOZLOV V G, BULOVIĆ V, BURROWS P E, *et al*.. Laser action in organic semiconductor waveguide and double-heterostructure devices[J]. *Nature*, 1997, 389(6649): 362-364.
[17] 李颜涛, 田玉冰, 刘星元. 电泵浦有机半导体激光器的关键技术[J]. 发光学报, 2009, 30(3): 414-416.
LI Y T, TIAN Y B, LIU X Y. Key techniques in electrically pumped organic semiconductor laser[J]. *Chinese Journal of Luminescence*, 2009, 30(3): 414-416. (in Chinese)
[18] ANDREW P, TURNBULL G A, SAMUEL I D W, *et al*.. Photonic band structure and emission characteristics of a metal-backed polymeric distributed feedback laser[J]. *Applied Physics Letters*, 2002, 81(6): 954-956.
[19] REUFER M, RIECHEL S, LUPTON J M, *et al*.. Low-threshold polymeric distributed feedback lasers with metallic contacts[J]. *Applied Physics Letters*, 2004, 84(17): 3262-3264.
[20] GIFFORD D K, HALL D G. Emission through one of two metal electrodes of an organic light-emitting diode via surface-plasmon cross coupling[J]. *Applied Physics Letters*, 2002, 81(23): 4315-4317.
[21] FENG J, OKAMOTO T, KAWATA S. Enhancement of electroluminescence through a two-dimensional corrugated metal film by grating-induced surface-plasmon cross coupling[J]. *Optics Letters*, 2005, 30(17): 2302-2304.
[22] BRUECK S R J, DIADIUK V, JONES T, *et al*.. Enhanced quantum efficiency internal photoemission detectors by grating coupling to surface plasma waves[J]. *Applied Physics Letters*, 1985, 46(10): 915-917.
[23] JIANG L Y, YIN T T, DUBROVKIN A M, *et al*.. In-plane coherent control of plasmon resonances for plasmonic switching and encoding[J]. *Light*: *Science* & *Applications*, 2019, 8(1): 21.

Author Biographics:

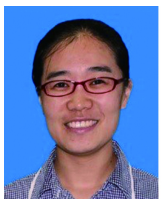

Yaoru Hao was born in Shijiazhuang, Hebei, in 1981. She received a Ph.D. degree in optics engineering in 2009 in the Changchun Institute of Optics, Fine Mechanics and Physics, Jilin, China. Her official title is Lecturer. Her research interests are in applied optics and computer simulation. E-mail:fengyunxiaohao@foxmail.com

Zhaoqi Deng was born in Yixing, Jiangsu, in 1981. He received an M.Sc. degree in optics engineering in 2007 in the Changchun Institute of Optics, Fine Mechanics and Physics, Jilin, China. His title is Lecturer. His research interests are in applied optics and computer simulation. E-mail: yeyunxiaopan@foxmail.com